Smart Structures and Systems, *Vol. 24, No. 4 (2019) 525-539*
DOI: https://doi.org/10.12989/sss.2019.24.4.525

Vibration characteristics of caisson breakwater for various waves, sea levels, and foundations

So-Young Lee[1a], Thanh-Canh Huynh[2b], Ngoc-Loi Dang[1c] and Jeong-Tae Kim*[1]

[1]Department of Ocean Engineering, Pukyong National Univ., 45 Yongso-ro, Nam-gu, Busan 48513, Republic of Korea
[2]Center for Construction, Mechanics and Materials, Institute of Research and Development, Duy Tan University, 03 Quang Trung, Hai Chau, Danang 550000, Vietnam

(Received February 20, 2019, Revised August 8, 2019, Accepted August 10, 2019)

Abstract. In this study, vibration characteristics of a gravity-based caisson-foundation breakwater system are investigated for ambient and geometric parameters such as various waves, sea levels, and foundation conditions. To achieve the objective, following approaches are implemented. Firstly, operational modal analysis methods are selected to identify vibration modes from output-only dynamic responses. Secondly, a finite element model of an existing caisson-foundation breakwater system is established by using a structural analysis program, ANSYS. Thirdly, forced vibration analyses are performed on the caisson-foundation system for two types of external forces such as controlled impacts and wave-induced dynamic pressures. For the ideal impact, the wave force is converted to a triangular impulse function. For the wave flow, the wave pressure acting on the system is obtained from wave field analysis. Fourthly, vibration modes of the caisson-foundation system are identified from the forced vibration responses by combined use of the operational modal analysis methods. Finally, vibration characteristics of the caisson-foundation system are investigated under various waves, sea levels, and foundations. Relative effects of foundation conditions on vibration characteristics are distinguished from that induced by waves and sea levels.

Keywords: caisson breakwater; wave-induced vibration response; various sea level; various foundation condition

1. Introduction

The gravity-based caisson breakwater resists to wave force by combined reaction behaviors of caisson and foundation. The breakwater structure is consistently damaged due to local and global variations of geometric and boundary properties deviated from its as-built state (Takagi 2015). Based on recent studies of the European coastline, the storm surge level and the wave climate become serious as compared to the design force of most of existing coastal structures (Galiatsatou *et al.* 2018). The gravity-based caisson breakwater becomes more vulnerable due to this reason, so that the integrity assessment becomes more important issue to the existing coastal structure.

For a reliable task of integrity assessment of a large constructed structure, the information of structural behaviors should be reliably analyzed and measured from numerical and experimental investigations (Kim and Stubbs 1995, Catbas *et al.* 2007). In the area of coastal infrastructure, there exist critical limitations for getting the structural information from the existing caisson breakwater. The first limitation is that most of the caisson-foundation system is submerged and only the top caisson region is exposed above the surface of the sea water. The second limitation is that the partially measurable structural responses of the top caisson may not represent the whole structural behaviors including the rigid caisson and the deformable foundation.

Vibration-based monitoring and structural identification is a promising way to overcome the above-mentioned difficulties, since dynamic responses measured by a few sensors on top of the caisson provide vibration characteristics of the entire system (Gul and Catbas 2011, Ho *et al.* 2012, Li *et al.* 2014, Shimoi *et al.* 2015). Utilizing the advantage of the vibration-based system identification, many researchers have investigated dynamic properties of the gravity-based breakwater system. Gao *et al.* (1988) performed forced vibration tests on a caisson breakwater to examine dynamic responses and vibration characteristics. Lamberti and Martinelli (1998) performed impact tests to investigate relative dynamic responses of a row of caissons by comparing the excited target and its adjacent ones. Cuomo *et al.* (2011) conducted laboratory tests on a small-scale caisson breakwater to analyze the stability of the system from measured dynamic responses and sliding distances under wave attack. Yi *et al.* (2013) performed tugboat impact tests on a caisson breakwater to in-situ analyze vibration characteristics such as natural frequency and modal damping. Huynh *et al.* (2019) also performed field tests on the same caisson breakwater to investigate the feasibility of system identification by using measured dynamic properties and a simplified numerical model.

Vibration characteristics of the breakwater system are affected by various ambient and geometric parameters such

*Corresponding author, Professor
E-mail: idis@pknu.ac.kr
[a] Ph.D.
[b] Ph.D.
[c] Ph.D. Student

http://www.techno-press.com/journals/sss&subpage=7
ISSN: 1738-1584 (Print), 1738-1991 (Online)

as various waves, sea levels, and foundation conditions. Lee *et al.* (2013) investigated vibration features of a lab-scale caisson-foundation system under two different excitation methods which include hammer impacts and ambient waves. Yi *et al.* (2014) performed field experiments on a caisson breakwater. Dynamic properties under tug boat collision and ambient waves were identified. Lee *et al.* (2015) analyzed effect of water level change and foundation damage on vibration characteristics for the lab-scale caisson-foundation system. Lee *et al.* (2018) performed vibration monitoring for a real caisson breakwater and analyzed dynamic behavior and effect of sea level on vibration features. Despite of those research efforts, there still remains a research need to examine the uncertainty of parameters of field vibration monitoring. The investigation of effect of each parameter is important to provide reliable results from field vibration monitoring.

In this study, vibration characteristics of a caisson-foundation breakwater system are investigated for ambient and geometric parameters such as various waves, sea levels, and foundation conditions. To achieve the objective, following approaches are implemented. Firstly, operational modal analysis methods are selected to identify vibration modes from output-only dynamic responses. Secondly, a finite element model of an existing gravity-based caisson breakwater is established by using a structural analysis program, ANSYS. Thirdly, forced vibration analyses are performed on the caisson-foundation system for two types of external forces such as controlled impacts and wave flow-induced dynamic pressures. For the ideal impact, the wave force is converted to triangular impulse function. For the wave flow, the wave pressure acting on the system is obtained from wave field analysis. Fourthly, vibration modes of the caisson-foundation system are identified from the forced vibration responses by combined use of the operational modal analysis methods. Finally, vibration characteristics of the caisson-foundation system are investigated under various waves, sea levels, and foundations. Relative effects of foundation conditions on vibration characteristics are distinguished from that induced by waves and sea levels.

2. Vibration analysis methods for submerged caisson-foundation system

2.1 Vibration monitoring condition

Submerged caisson-foundation system has limitations on placing sensors and implementing excitations for vibration monitoring. Since it is mostly submerged under sea water, only the top of the caisson is accessible for field measurement which requires dry condition. As shown in Fig. 1, a caisson breakwater is placed on a rubble mound and armored by a protection unit. Then it receives pulsating wave loads from incident waves. Once the wave induces the excitation on the rigid caisson which is placed on the deformable foundation including rubble mound and sea bed, it produces integrated vibration responses of the caisson-foundation system.

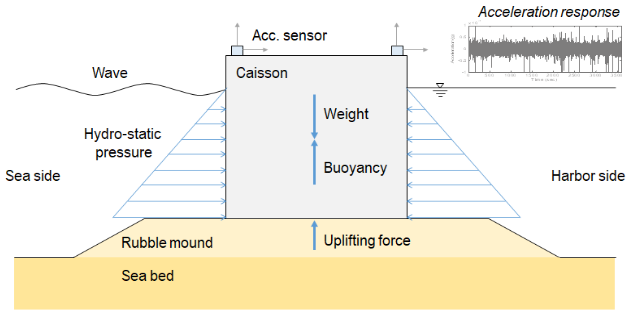

Fig. 1 Vibration monitoring condition of submerged caisson-foundation system

A structural system is represented by structural dynamic characteristics such as stiffness, mass, and damping properties. Its acceleration responses depend on the structural characteristics and it can be defined as

$$\ddot{u}_t = [\mathrm{M}]^{-1}(\{F\} - \dot{u}_t[\mathrm{C}] - u_t[\mathrm{K}]) \tag{1}$$

in which u_t, $\dot{u}_t$, $\ddot{u}_t$ represent the displacement, velocity, and acceleration vectors, respectively; [M], [K] and [C] represent the mass matrix, stiffness matrix, and damping matrix, respectively; and {F} is the vector of external wave forces.

The acceleration response provides information of the dynamic structural parameters that may be feasible for structural integrity assessment. In field practice, it is very hard to estimate the input wave load {F} acting on the target structure, so that the available information, in most cases, is limited as the output vibration response (e.g., acceleration signal $\{\ddot{u}\}$ of the caisson breakwater). For the forced response of a damped structural system, the general receptance frequency response function (FRF) can be simplified in a complex form as follows (Ewins 2000)

$$\mathrm{FRF}(\omega) = ([\mathrm{K}] + i\omega[\mathrm{C}] - \omega^2[\mathrm{M}])^{-1} \tag{2}$$

in which the FRF is defined as a force to displacement response ratio in a frequency domain. As Eq. (1) can be equivalently interpreted as Eq. (2), the system's dynamic characteristics can be estimated via modal parameters such as natural frequency, modal damping and mode shape.

2.2 Output-only modal analysis methods

For ambient condition like stochastic random excitation, the system's acceleration signals are output-only (i.e., unknown input force) vibration responses. To extract modal parameters from output-only vibration responses, modal analysis can be performed in time-domain or frequency-domain. In this study, a combined approach with time-domain and frequency-domain methods was selected to experimentally estimate modal parameters such as natural frequency, modal damping and mode shape of the caisson-foundation system. As the time-domain method, we selected the stochastic subspace identification (SSI) method (Overschee and De Moor 1996). As the frequency-domain method, we also selected the frequency domain decomposition (FDD) method (Brinker *et al.* 2001). According to a comparative study by Yi and Yun (2004), those two methods showed good performances in terms of the accuracy, the computational time and the simplicity.

The FDD method is a frequency domain technique that decomposes the spectral density function matrix and generates a set of single degree of freedom systems from the response (Brinker *et al.* 2001). The procedure of the FDD method is summarized in two steps. First, a set of output responses from n sensors on a structure is acquired. Next, the power spectral density (PSD) matrix is calculated as follows

$$\boldsymbol{S}_{yy}(\omega) = \begin{bmatrix} S_{11}(\omega) & S_{21}(\omega) & \cdots & S_{1n}(\omega) \\ S_{21}(\omega) & S_{22}(\omega) & & S_{2n}(\omega) \\ \vdots & & \ddots & \vdots \\ S_{n1}(\omega) & S_{n2}(\omega) & \cdots & S_{nn}(\omega) \end{bmatrix} \tag{3}$$

where the $\boldsymbol{S}_{yy}(\omega)$ is the PSD matrix. In Step 3, the PSD matrix by using the singular value decomposition (SVD) algorithm as follows

$$\boldsymbol{S}_{yy}(\omega) = \mathbf{U}(\omega)^{\mathrm{T}}\Sigma(\omega)\mathbf{V}(\omega) \tag{4}$$

where $\sum(\omega)$ is a diagonal matrix containing the singular values $\sigma_i(\omega)$ (i = 1, 2, … n) of its PSD matrices, $\mathbf{U}(\omega)$ and $\mathbf{V}(\omega)$ are unitary matrices. The $\mathbf{U}(\omega)$ matrix equals the $\mathbf{V}(\omega)$ matrix since $\boldsymbol{S}_{yy}(\omega)$ is symmetric. In Step 4, peak frequencies (i.e., natural frequency ω_{n}) are identified in the first singular value $\sigma_i(\omega)$. In Step 5, the mode shapes are extracted from any of column vectors of $\mathbf{U}(\omega)$ at the corresponding peak frequencies (Brinker *et al.* 2001, Yi and Yun 2004).

The SSI method is a time domain technique that involves complicated mathematic description (Brinker and Andersen 2006). The SSI method can be described in five steps based on existing studies (Lee *et al.* 2018). Firstly, the cross-correlation matrices are calculated from the measured time signals. Secondly, the Hankel matrix [**H**] is constructed from the obtained correlation matrices as Eq. (5). Thirdly, the invertible weighting matrices $\mathbf{W}_1$ and $\mathbf{W}_2$ are pre- and post-multiplied to the Hankel matrix. Then, this matrix is decomposed into the observability $\boldsymbol{\mathcal{O}}_{n1}$ and the system matrix **A** as Eq. (6).

$$\mathbf{H}_{n_1 n_2} = \begin{bmatrix} \mathbf{R}_1 & \cdots & \mathbf{R}_{n_2} \\ \vdots & \ddots & \vdots \\ \mathbf{R}_{n_1} & \cdots & \mathbf{R}_{n_1+n_2-1} \end{bmatrix} \tag{5}$$

$$\begin{aligned} \mathbf{W_1 H W_2} &= [\mathbf{U_1}\ \ \mathbf{U_2}] \begin{bmatrix} \Sigma_1 & \mathbf{0} \\ \mathbf{0} & \mathbf{0} \end{bmatrix} \begin{bmatrix} \mathbf{V}_1^{\mathrm{T}} \\ \mathbf{V}_2^{\mathrm{T}} \end{bmatrix} \\ &\approx \mathbf{U_1}\Sigma_1\mathbf{V}_1^{\mathrm{T}} \Leftrightarrow \mathbf{W_1}\, \boldsymbol{\mathcal{O}}_{\mathbf{n1}}\boldsymbol{\mathcal{O}}_{\mathbf{n2}}\mathbf{W_2} \end{aligned} \tag{6}$$

where **U**, **V** and $\sum_1$ are the unitary matrices and the singular value matrix respectively. The system matrix **A** is obtained from the observability matrix $\boldsymbol{\mathcal{O}}_{n1}$. Fourthly, the eigenvalues μ and the eigenvectors ψ of the system are computed by decomposing the system matrix A as Eq. (7).

$$\begin{gathered} \mathbf{A\Psi} = \mathbf{\Psi M} \\ (\mathbf{M} = \mathrm{diag}(\mu_1, \mu_2, \dots, \mu_N) \in \mathbf{R}^{N\times N}, \\ \mathbf{\Psi} = [\psi_1, \psi_2, \dots, \psi_N] \in \mathbf{R}^{N\times N}) \end{gathered} \tag{7}$$

Finally, several criteria are applied to classify stable modes, unstable modes and noise modes. Then a proper system order is decided via the Stabilization chart (Yi and Yun 2004, Brinker and Andersen 2006).

3. Numerical modelling of a real caisson breakwater

3.1 Description of target structure

The Oryuk-do caisson breakwater (which is located in Busan, Korea) was selected for the numerical study. As shown in Fig. 2(a), the breakwater protects the port of Busan from severe incident waves of the south-east direction. As shown in Fig. 2(b), the breakwater system of a total length of 1,004m consists of 50 caisson units. The geometry and sectional dimensions of the target structure are described in Fig. 3. Caisson units are partially submerged in sea water and only top of the caisson is exposed to the air. It means that only top of the caisson is accessible for installation of vibration sensors. Each caisson unit has 20 m in width, 20 m in length and 20.78 m in height including cap concrete of 4m tall. Caisson units #4 - #47 have parapets of 5.3 m in height and 8.8 m. The caisson stands on mainly three foundation layers which are rubble mound, sand-fill ground, and natural ground. The details of dimension and description for the target structure are presented in Huynh *et al.* (2019).

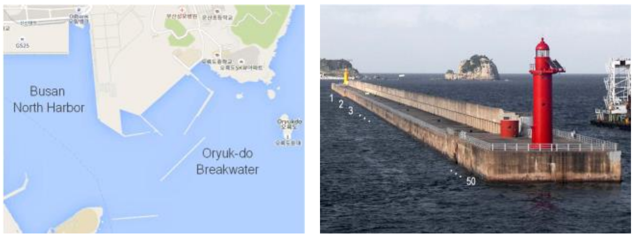

(a) Google map (b) Site view

Fig. 2 The Oryuk-do breakwater of the port of Busan, Korea

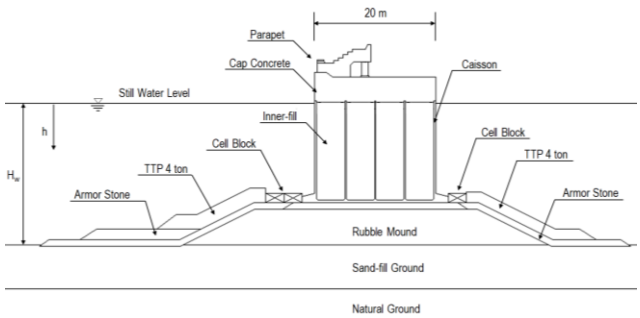

Fig. 3 Geometry and sectional dimensions of the Oryuk-do breakwater system

3.2 Finite element model of caisson-foundation system

Huynh *et al.* (2019) introduced a numerical model to analysis dynamic behavior of a caisson-foundation system. As shown in Fig. 4, a finite element (FE) model of the target caisson structure was simulated using ANSYS software. Among whole breakwater structure, a single caisson unit was considered with certain limitation on geometric and boundary conditions. The FE model consists of five element groups: cap concrete, caisson, armor stone, rubble, and sand-fill. Material properties of those layer-by-layer element groups were selected as outlined in Table 1. Elastic properties of the cap concrete and the caisson are based on concrete design strength, and caisson filler. Elastic properties of the rubble mound and the sea bed (dense sand-fill) are based on the experimental guideline by Bowles (1996) and the previous reports on the Oryuk-do caisson breakwater by Yi *et al.* (2013). A caisson-foundation system is modeled by assuming that the sand-fill layer' bottom boundary is constraint and the interlocking between adjacent caisson units is not allowed for motions of all DOFs.

Solid elements were mostly used for modeling the caisson-foundation system. Some parts like parapet structure, TTP, and cell block were simulated by nodal masses. The submerged condition was simulated by adding the effective mass of sea water. It is noted that hydrodynamic damping with respect to sea water was not considered in this simulation study. Westergaard's hydrodynamic water pressure equation, Eq. (8), was used to calculate the effective mass of sea water. In Eq. (8), M_w is the hydrodynamic mass, ρ_w is the seawater density as 1027 kg/m^3, H_w is the depth from water level to foundation and h is the depth from the still water level to the action point of hydrodynamic pressure. The water depth H_w was selected as 22.19m on the basis of the site information (Lee *et al.* 2019).

$$M_w = \int_{h_1}^{h_2} \frac{7}{8} \rho_w \sqrt{H_w h}\, dh \quad (8)$$

Table 1 Material properties of FE model (Lee *et al.* 2019)

	Elastic modulus (MPa)	Poisson's ratio	Mass density (kg/m^3)	Spring constant (kg/m/m^2)
Cap Concrete	2.80E+04	0.2	2.50E+03	-
Caisson	2.80E+04	0.2	2.08E+03	-
Armor Stone	140	0.3	1.50E+03	-
Rubble mound	140	0.3	2.10E+03	-
Sand Fill	66.5	0.325	1.62E+03	-
Natural Ground	-	-	-	1.25E+07

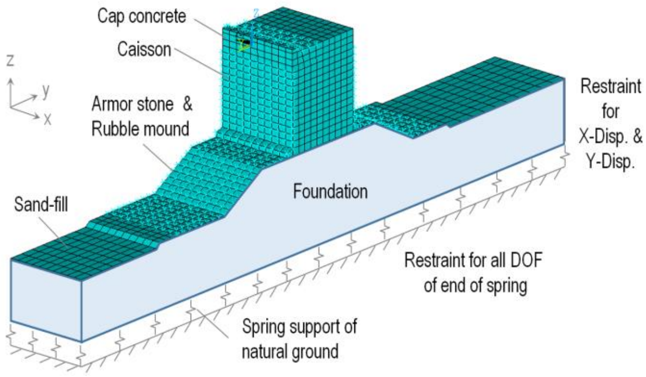

(a) FE modeling of subsystems

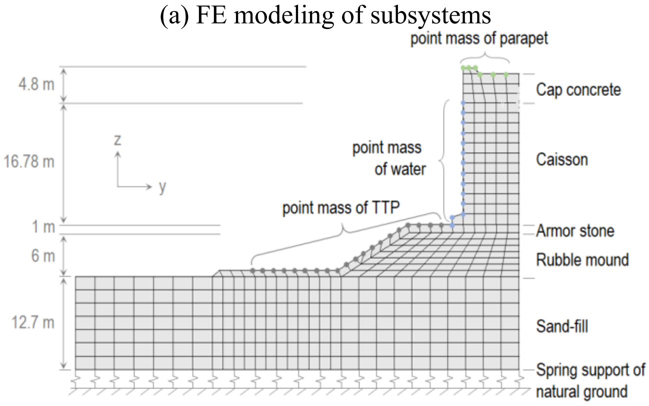

(b) Details of FE model

Fig. 4 FE model of caisson-foundation system (Lee *et al.* 2019)

4. Analysis of vibration characteristics of caisson-foundation system

4.1 Free vibration analysis for modal parameter identification

Free vibration analyses of the caisson-foundation system were performed to identify modal parameters like mode shapes and natural frequencies. It is noted that the caisson-foundation system has complex vibration motions out of caisson's rigid motion and foundation's deformable motion. The foundation motions are deformation modes corresponding to caisson rigid body motions. From the FE analysis, totally ten vibration modes were extracted in 3Hz low-pass frequency band as outlined in Table 2. The subscript 'Fr' indicates the vibration modes identified from free vibration analysis. Mode Fr 1 is a combined vibration mode of caisson's pitching motion with respect to y-axis and foundation's twisting motion (see Fig. 5(a)). Mode Fr 2 is a complex mode of caisson's rolling motion with respect to x-axis and foundation's bending motion (see Fig. 5(b)). Mode Fr 3 is a complex mode of caisson's heaving motion and foundation's vertical expansion motion (see Fig. 5(c)). Mode Fr 4 is a complex mode of caisson's rolling motion with respect to x-axis and foundation's bending motion with respect to x-axis (see Fig. 5(d)). As outlined in Table 2, Mode Fr 5 - Mode Fr 9 are complex modes of caisson's rolling motions and foundation's bending motion. Also,

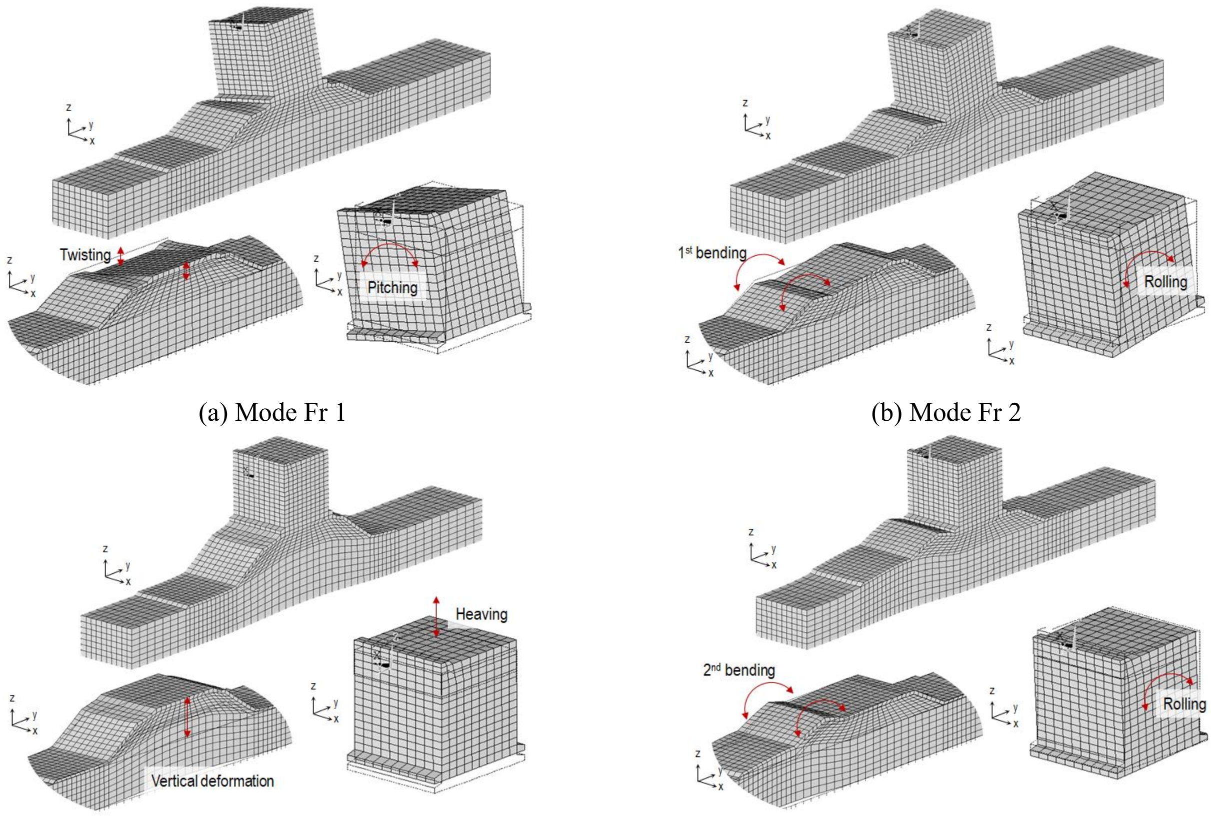

(a) Mode Fr 1 (b) Mode Fr 2

(c) Mode Fr 3 (d) Mode Fr 4

Fig. 5 Complex modes from free vibration analysis of caisson-foundation system

Table 2 Free vibration modes and natural frequencies of caisson-foundation system

Mode	Natural Frequency (Hz)	Caisson's motion	Foundation's motion
Mode Fr 1	1.3784	Pitching w.r.t. y-axis	Twisting
Mode Fr 2	1.5120	Rolling w.r.t. x-axis	Bending w.r.t. x-axis
Mode Fr 3	1.6475	Heaving	Vertical expanding
Mode Fr 4	2.5862	Rolling w.r.t. x-axis	Bending w.r.t. x-axis
Mode Fr 5	2.7042	Rolling w.r.t. x-axis	Bending w.r.t. x-axis
Mode Fr 6	2.8084	Rolling w.r.t. x-axis	Bending w.r.t. x-axis
Mode Fr 7	2.8446	Rolling w.r.t. x-axis	Bending w.r.t. x-axis
Mode Fr 8	2.8934	Rolling w.r.t. x-axis	Bending w.r.t. x-axis
Mode Fr 9	2.9376	Rolling w.r.t. x-axis	Bending w.r.t. x-axis
Mode Fr 10	3.0253	Pitching w.r.t. y-axis	Twisting

Mode Fr 10 is a complex mode of caisson's pitching motion and foundation's twisting motion.

4.2 Feasibility of wave-induced vibration monitoring

The feasibility of monitoring wave-induced vibration responses was examined by implementing ideal wave impacts to the caisson-foundation system. Wave impacts were simulated as triangular impulses that were applied to the front wall at the still water level. Schmidt *et al.* (1992) defined wave impact force ($F_{h,\max}$) by the wave height (H_b), wave period (T_p), and duration time (t_d) as

$$F_{h,\max} = 1.24\rho_w g H_b^2 \left(t_d/T_p\right)^{-0.344} \tag{9}$$

where ρ_w is the density of sea water and g is the gravitational acceleration.

As indicated in Fig. 6, the wave impact force was calculated for the wave height of 6m and the wave period of 15s. The maximum wave force ($F_{h,\max}$) and the duration time (t_d) was calculated as 13,422 kN/m and 12ms, respectively. The ratio of the rise time (t_r) to the total peak

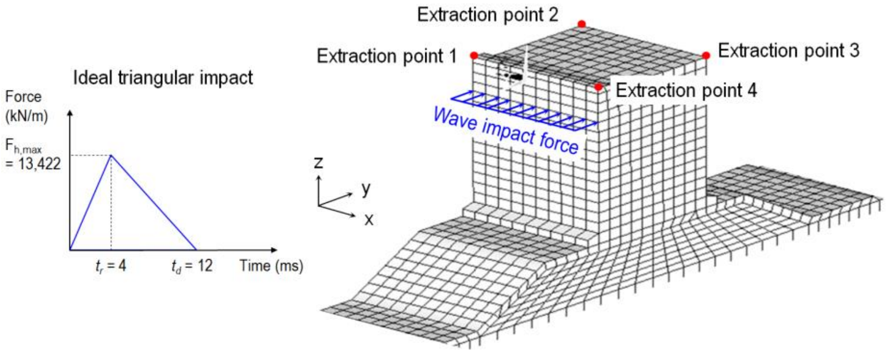

Fig. 6 Simulation of ideal wave impact for forced vibration analysis

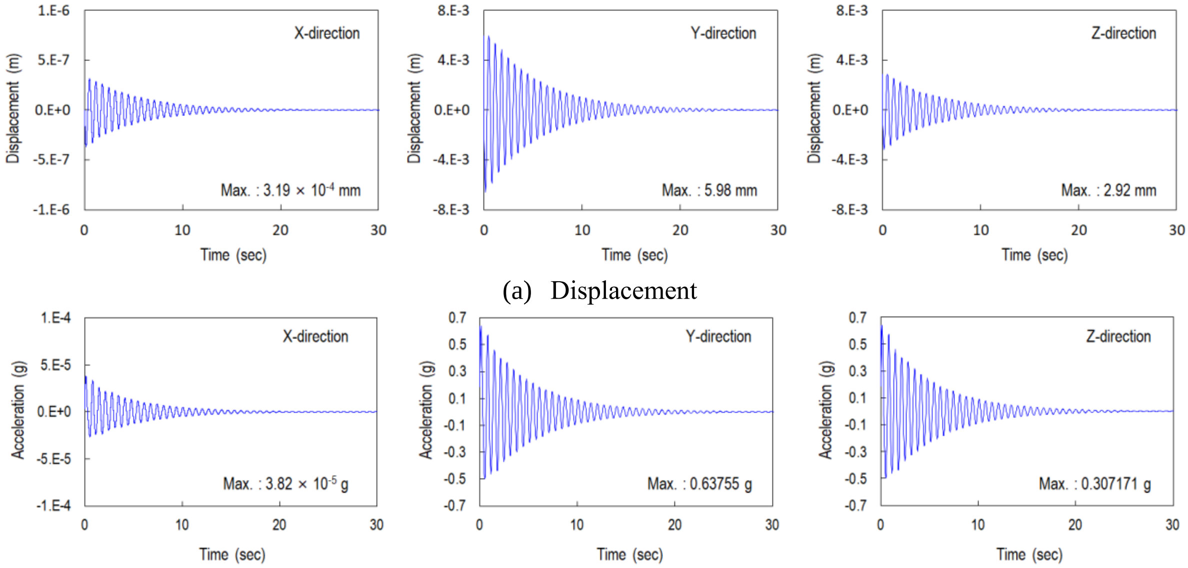

(a) Displacement

(b) Acceleration

Fig. 7 Horizontal vibration responses at Extraction point 1 for ideal wave impact

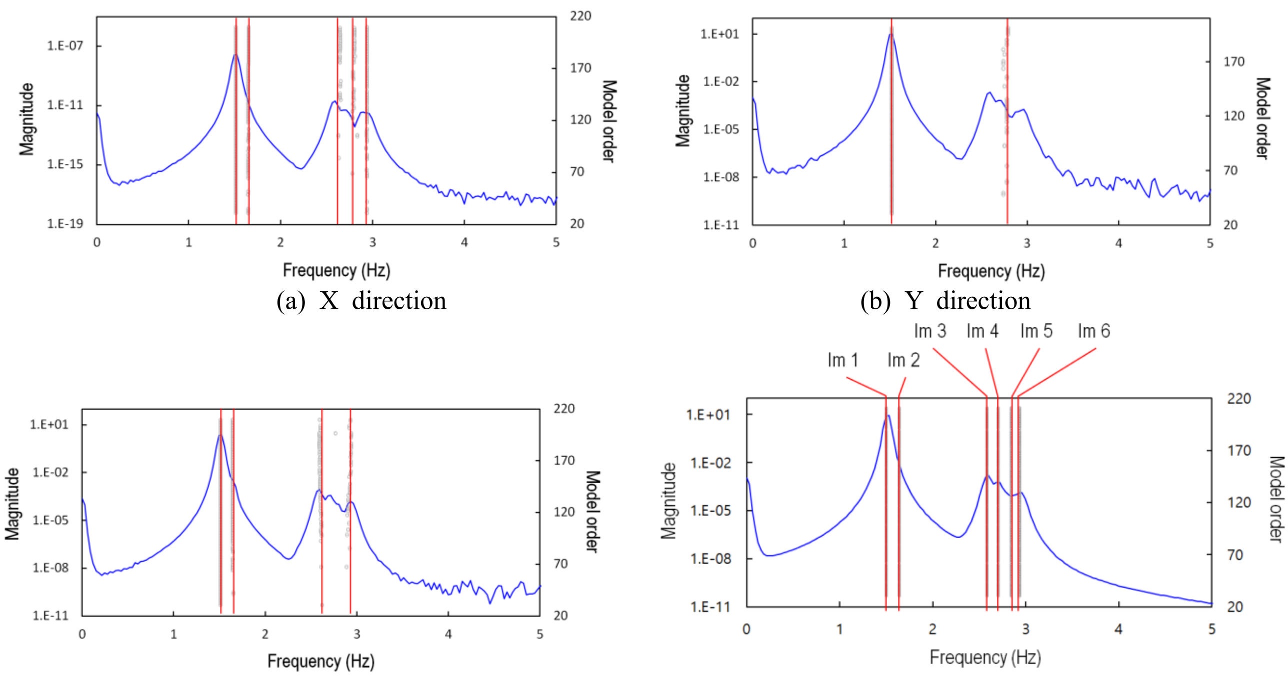

(a) X direction

(b) Y direction

(c) Z direction

(d) All directions

Fig. 8 Frequency responses and modal identification for ideal wave impact

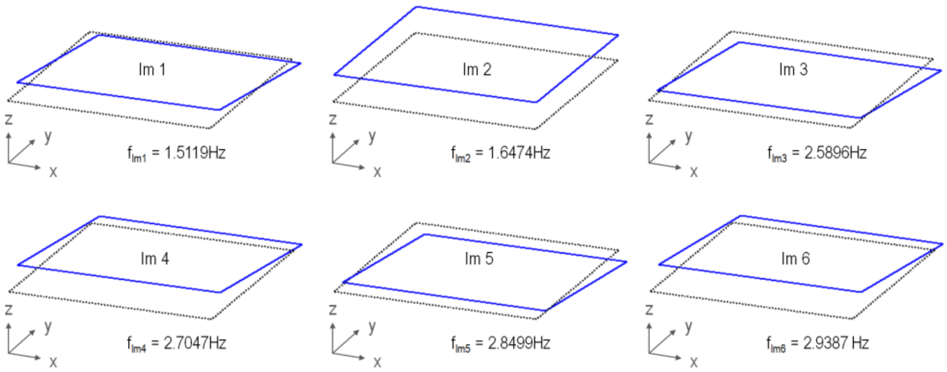

Fig. 9 Six mode shapes of forced vibration analysis under ideal wave impact

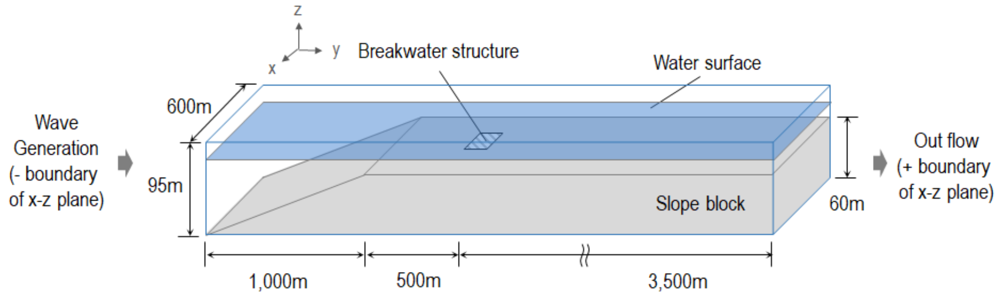

(a) Wave field modeling

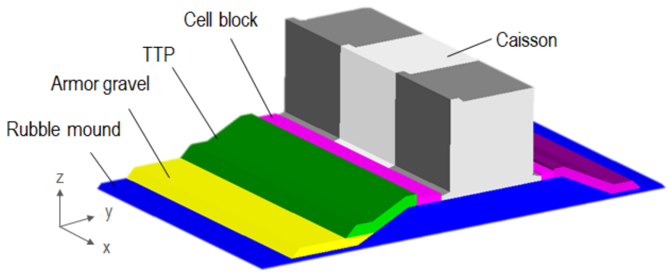

(b) Breakwater structure of wave field

Fig. 10 Numerical modeling of wave field for wave pressure simulation

duration (t_d) was found to vary between 0.3 and 0.65, depending on the amount of trapped air and the magnitude of the force peak (Vink 1997). In this analysis t_r/t_d was assumed as 0.33 and the rise time was calculated as 4ms.

The wave impact force was applied to the front wall at the still water level in y-direction (see Fig. 6). Modal damping ratio was defined as 2% on the basis of modal damping ratio from field experiment on the target structure (Lee *et al.* 2018). Considering the on-site accessibility, vibrational responses were extracted from the four points at the top of the caisson. The sampling frequency was set as 50Hz for the controlled impact excitation. As shown in Fig. 7, vibration responses in y-direction were larger than those in two other directions. The maximum displacement was 5.98 mm (Fig. 7(a)) and the maximum acceleration was 0.64 g (Fig. 7(b)).

Modal parameters were identified from the combined use of the FDD and SSI methods. As shown in Fig. 8(a), five modes were identified from single x directional acceleration responses. As also shown in Figs. 8(b) and 8(c), two and four modes were identified from individual y and z directional responses, respectively. It is noted that any single directional responses may not guarantee to identify enough vibration modes. Fig. 8(d) shows mode identification results by using all three directional responses together, from which six modes were identified under the wave impact force. The subscript 'Im' indicates the vibration modes obtained from the ideal triangular impact.

Next, mode shapes were extracted for the six identified mode as shown in Fig. 9. Mode Im 1 was matched to Mode Fr 2 (see Fig. 5(b)), representing the caisson's rolling motion and the foundation's bending motion. Mode Im 2 was matched to Mode Fr 3 (see Fig. 5(c)), representing the caisson's heaving motion and the foundation's vertical

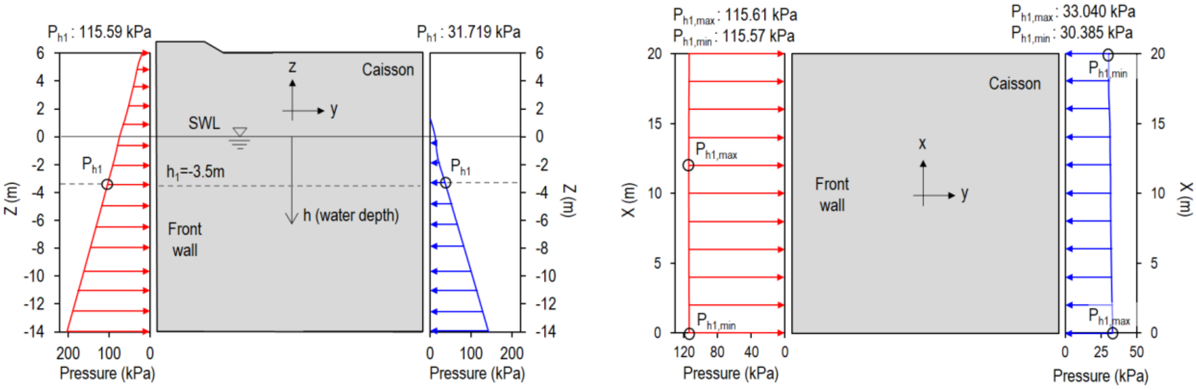

(a) Vertical distribution of pressure (b) Pressure at h_1 = -3.5 m

Fig. 11 Wave pressures acting on front and back walls for Wave 1

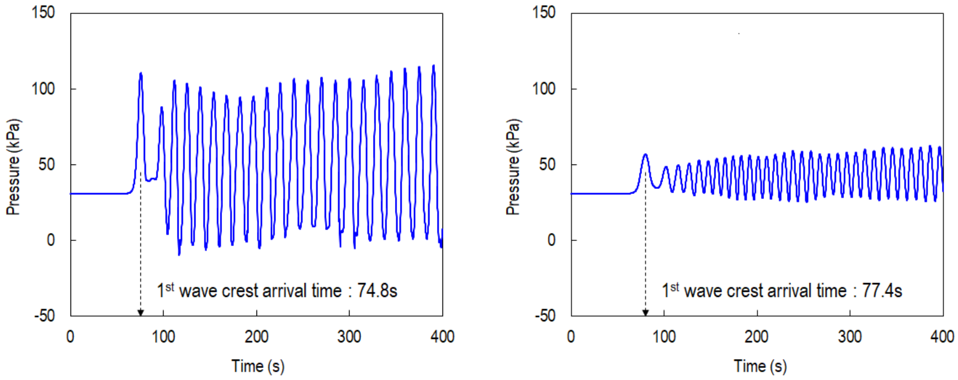

(a) Wave 1 (b) Wave 5

Fig. 12 Time history of dynamic wave pressure acting on front wall at h_1 (-3.5 m)

expansion motion. Mode Im 3 was matched to Mode Fr 4 (see Fig. 5(d)), representing the caisson's rolling motion and the foundation's bending motion. Last three modes (i.e., modes Im 4 – Im 6) were matched to Mode Fr 5, Mode Fr 7 and Mode Fr 9 (see Table 2), respectively. It is noted that Fr 1 (see Fig. 5(a) representing the caisson's pitching motion and the foundation's twisting motion) was not identified from the forced vibration analysis.

5. Numerical analysis of vibration characteristics from wave-induced dynamic pressure

5.1 Simulation of dynamic wave pressure on caisson-foundation system

5.1.1 Wave field analysis

As illustrated in Fig. 10(a), a numerical modeling of wave field was implemented. The wave field was simulated of as follows: 5000 m in length, 600 m in width, and 95 m in height. The dimensions were determined to minimize the influence of reflecting waves at the out flow boundary. The breakwater structure was located at 1500 m far from wave generating plane. The slope block was employed to achieve intended waves at the area of the breakwater structure effectively as the incident wave propagated in the y-direction. As shown in Fig. 10(b), the structure consists of three caissons, cell block, TTP, armor gravel, and rubble mound modeled by impermeable block. Three caissons were considered to reduce vortex effects at the corner of the caissons and the pressure data were achieved from the middle caisson.

5.1.2 Wave-induced dynamic pressure

Dynamic wave scenarios were selected based on design wave of Oryuk-do breakwater and wave height records at Gyoboncho tidal station (KHOA 2019). Wave 1 is on the design wave height and period of the Oryuk-do caisson breakwater. Wave 5 represents the normal wave condition of the Oryuk-do caisson breakwater. Waves 2-4 are potential wave conditions between Wave 1 and Wave 5. As shown in Fig. 11, the wave pressures acting vertically to the front and back walls were analyzed for the three waves. Among the waves, Wave 1 was the biggest wave with 6m wave height and 15s wave period, and Wave 5 was the smallest wave with 1.5m wave height and 8s wave period. For Wave 1, the vertical distribution of the wave pressure was calculated at the front and back walls (see Fig. 11).

Table 3 Wave pressures simulated at h_1 (-3.5 m) for three wave cases

Cases	Wave height (m)	Wave period (s)	Max. wave pressure at h_1 (kPa)
Wave 1	6	15	115.59
Wave 2	4.9	13.3	96.80
Wave 3	3.8	11.5	77.61
Wave 4	2.6	9.8	68.02
Wave 5	1.5	8	62.42

Table 4 Vibration modes identified from three different vibration analyses

Excitation condition	Free vibration	Ideal wave impact	Wave dynamic pressure
Identified mode (Frequency)	Fr 1 (1.378 Hz)	-	-
	Fr 2 (1.512 Hz)	Im 1 (1.512 Hz)	Wp 1 (1. 493 Hz)
	Fr 3 (1.648 Hz)	Im 2 (1.648 Hz)	-
	Fr 4 (2.586 Hz)	Im 3 (2.590 Hz)	Wp 2 (2.549 Hz)
	Fr 5 (2.704 Hz)	Im 4 (2.705 Hz)	Wp 3 (2.664 Hz)
	Fr 6 (2.808 Hz)	-	-
	Fr 7 (2.845 Hz)	Im 5 (2.850 Hz)	-
	Fr 8 (2.893 Hz)	-	-
	Fr 9 (2.938 Hz)	Im 6 (2.939 Hz)	-
	Fr 10 (3.025 Hz)	-	-

A certain water depth h_1=-3.5 m (e.g., about the half of the biggest wave height) was selected to fairly examine the height 6m and wave period 15s), the first wave crest arrived at 74.8s to the front wall and it occurred the maximum pressure 115.59kPa at h_1 (see Fig. 12(a)). In Wave 5 (i.e., wave height 1.5m and wave period 8s), the first wave crest arrived at 77.4s and it occurred the maximum pressure 62.42kPa at h_1 (see Fig. 12(b)). For the five wave scenarios, the pressures at h_1 (h=-3.5 m) were investigated as outlined in Table 3. The pressure was decreased with respect to the decrease of the wave height and the wave period.

5.2 Estimation of wave-induced vibration responses and modal parameters

As shown in Fig. 13, wave-induced vibration responses of the caisson-foundation system were analyzed for Wave 1. Under the dynamic wave pressures shown in Fig. 13, displacement and acceleration responses were fluctuated with respect to the wave propagation. Maximum wave pressures for all wave scenarios.

As shown in Fig. 11(a), the vertical pressure distribution is almost linear at the front and back walls. At the water depth h_1, the pressures (P_{h1}) were calculated as 115.59kPa at the front wall and 31.719kPa at the back wall when the wave crest was occurred at the front wall. As shown in Fig. 11(b), the laterally distributed pressures of the front wall were examined from 115.57kPa to 115.61kPa along the x direction. The pressure at the back wall was distributed from 30.385kPa to 30.040kPa. It is noted that the lateral pressure distributions were almost uniform for both of the walls. It is also noted that the pressure distribution of the middle breakwater may not be linear at both later edges due to vortex effect at the corner of the breakwater.

Dynamic pressures of the two waves (i.e., Wave 1 and Wave 5) were compared in Fig. 12. In Wave 1 (i.e., wave displacement and acceleration were 23.2 mm and 1.4 g, respectively. Vibration responses in y-direction were larger than those of two other directions.

For Wave 1, modal parameters were extracted from the acceleration responses by the combined use of the FDD and SSI methods. All three directional responses were used to extract modal parameters, as shown in Fig. 14. As shown in Fig. 14(a), three vibration modes were identified from the frequency response. As shown in Fig. 14(b), all modes were identified as rolling motions. The subscript 'Wp' indicates the vibration modes obtained from the wave-induced dynamic pressure.

Table 4 outlines identified modes from the three different vibration analyses, which are the free vibration analysis (see Fig. 5 and Table 2), the forced vibration analysis under the ideal wave impact (see Fig. 9), and the forced vibration analysis under the wave dynamic pressure (see Fig. 14). From the comparison, Mode Wp1 was matched to Mode Im 1 (which is identical to Mode Fr 2 in Fig. 5(b)). Mode Wp 2 was matched to Mode Im 3 (which is identical to Mode Fr 4 in Fig. 5(d)). Mode Wp 3 was matched to Mode Im 4 (which is identical to Mode Fr 5 in Table 2).

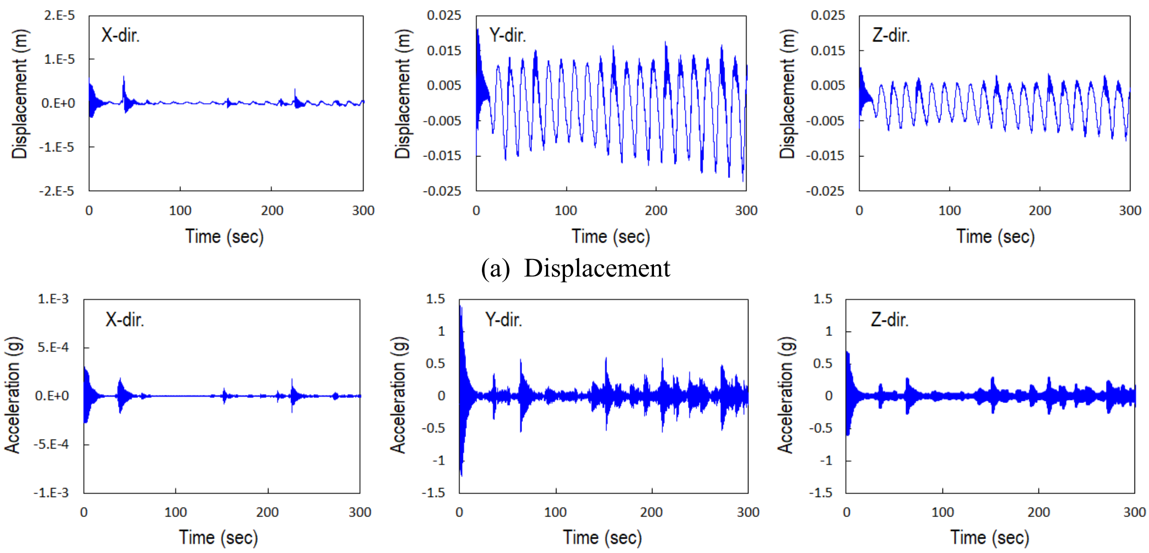

(a) Displacement

(b) Acceleration

Fig. 13 Vibration responses at Extraction point 1 under Wave 1 dynamic pressure

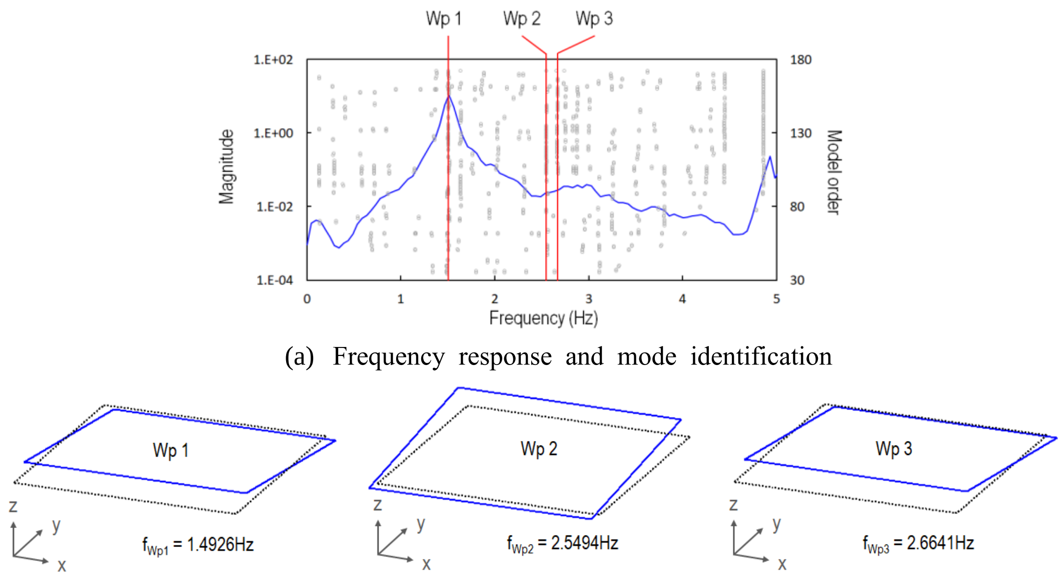

(a) Frequency response and mode identification

(a) Three mode shapes under wave-induced pressures

Fig. 14 Frequency responses and modal identification for Wave 1 dynamic pressures

6. Vibration characteristics under various waves, sea levels, and foundations

In this section, vibration characteristics of the caisson-foundation system were investigated under various waves, sea levels, and foundations. Firstly, the effect of various waves on vibration characteristics was analyzed. Secondly, the effect of various sea levels on vibration characteristics was analyzed. Thirdly, the effect of various foundation conditions on vibration characteristics was analyzed.
Finally, the relative effect of foundation conditions on vibration characteristics was distinguished from that induced by waves and sea levels.

6.1 Effects of various waves on vibration characteristics

Five different wave conditions, as previously described in Table 3, were considered to examine the variation of vibration characteristics due to the variation of wave height and period. As noted, all five wave scenarios were selected based on design wave of Oryuk-do breakwater and wave height records at Gyoboncho tidal station (KHOA 2019). As also listed in Table 5, wave pressures were calculated for the five wave cases, for which the wave pressure was varied gradually with respect to the wave size. It is noted that sea level was assumed to be same in the forced vibration

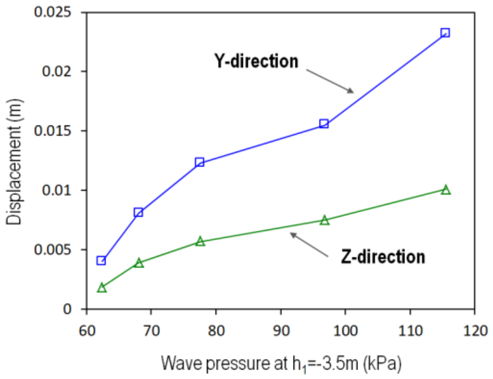

(a) Displacement

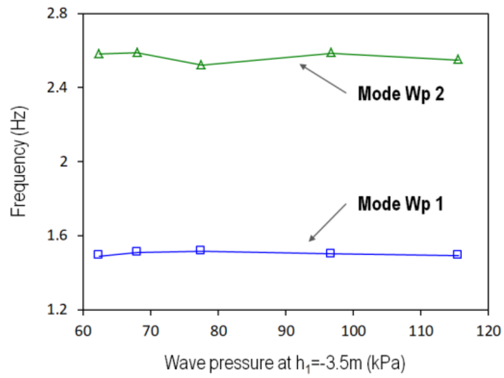

(b) Natural frequency

Fig. 15 Displacement variation at top of caisson and natural frequency due to wave pressure variation

Table 5 Vibration characteristics of caisson-foundation system under various wave pressures

Cases	Wave pressure* (kPa)	Max. displacement (mm)**		Natural frequency (Hz)	
		Y-dir.	Z-dir.	Mode Wp 1	Mode Wp 2
Wave 1	115.59	23.2	10.1	1.4926	2.5494
Wave 2	96.80	15.5	7.5	1.5027	2.5847
Wave 3	77.61	12.3	5.7	1.5179	2.5206
Wave 4	68.02	8.1	3.9	1.5117	2.5895
Wave 5	62.42	4.0	1.9	1.4922	2.5816

* Wave pressures were obtained from the caisson front wall at h_1=-3.5 m.

** Maximum displacements were obtained from Extraction point 1 (see Fig. 6).

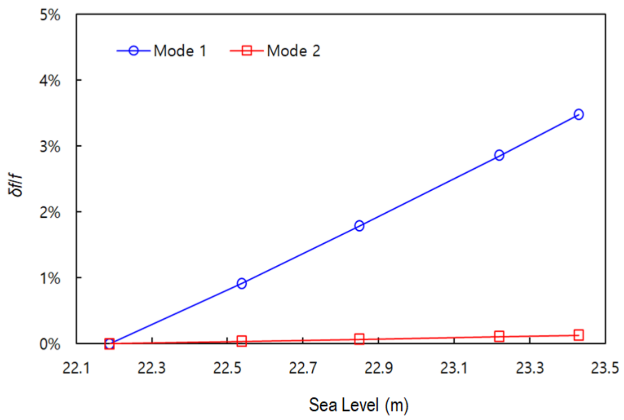

Fig. 16 Variation rate of natural frequencies due to sea level change

Table 6 Variation of displacement and natural frequency with respect to sea level change

Case	Sea level (H_w)	Max. displacement (mm)	Natural frequency (Hz)	
			Mode Im 1	Mode Im 3
1	23.43 m	5.67	1.4864	2.5846
2	23.22 m	5.72	1.4909	2.5849
3	22.85 m	5.81	1.4987	2.5854
4	22.54 m	5.89	1.5051	2.5858
5	22.19 m	5.98	1.5120	2.5862

analysis for each wave conditions. As previously described in Fig. 13(a), displacement signals were extracted from forced vibration analysis under the wave-induced dynamic pressure. Acceleration signals were calculated from the displacement signals, and mode identification was performed by the operational modal analysis (i.e., the combined use of the FDD and SSI methods). Two modes Wp 1 and Wp 2 were extracted from the mode identification.

As shown in Fig. 15(a) and also listed in Table 5, maximum displacements in y-direction and z-direction were analyzed for the five wave cases. The maximum displacement was increased gradually due to the increment of the wave size. In Wave 1, the y-directional displacement was about 2.86 times of Wave 5. The z-directional displacement was about 5.32 times of Wave 5. The variation of the z-directional displacement was relatively bigger than the y-direction. As shown in Fig. 15(b) and also listed in Table 5, the variations of natural frequencies of the two modes were analyzed for the five wave cases. Natural frequencies were slightly changed irregularly, with the maximum variation of 3.5% in Mode Wp 1 and 5.5% in Mode Wp 2. It means that natural frequency will be varying 3.5~5.5% when the target caisson-foundation system experience up to design wave. It is observed that the variation of wave-induced pressures has little effect on natural frequencies of the two rolling vibration modes of the caisson-foundation system.

6.2 Effects of various sea levels on vibration characteristics

To examine the effect of sea level changes, vibration characteristics were relatively analyzed for different sea levels. Five sea levels were considered as described in Table 6. Based on tide records at Busan Tidal Station (KHOA 2019), water levels of highest and lowest sea levels were selected as 23.43 m and 22.19 m, respectively. It notes that variation range of the scenario of sea level was corresponding to tidal range of one day. For the sea level simulation, added mass of water (which can be calculated by Westergaard's equation (Westergaard 1933)) was applied to the FE model.

Forced vibration analysis with wave impact force was performed for each scenario to extract displacement signals of the caisson-foundation system. The horizontal displacement was extracted from Extraction point 1 and listed in Table 6. Displacements were slightly and gradually increased due to decrease of the sea level. It notes that decrease of sea level induce decrease of mass effect and lead to increase of displacement.

From wave impact simulation, Modes Im 1 and Im 3 (which are identical to Modes Wp 1 and Wp 2) were extracted by the combined use of the FDD and SSI methods. As listed in Table 6 and described in Fig. 16, natural frequencies of modes Im 1 and Im 3 were increased due to the sea level decrease. Fig. 16 shows the variation rate of natural frequency due to the change of sea level. For the tidal range of one day, natural frequencies were changed up to 3.4% in Mode Im 1 and only 0.1% in Mode Im 3. It is observed that the sea level change mainly contributes to Mode Im 1 and slightly affects to Mode Im 3. It is also noted that Mode Im 1 is the first complex mode of the caisson's rolling and the foundation's flexural motions and Mode Im 3 is the second complex mode of the caisson's rolling and the foundation's flexural motions.

6.3 Effects of various foundation conditions on vibration characteristics

6.3.1 Vibration characteristics under various foundations

Seven stiffness decrease scenarios, as outlined in Table 7, were considered to examine the variation of vibration characteristics due to the variation of foundation properties. The foundation of the caisson-foundation system includes armor stone, rubble mound, sand fill and natural ground. So the stiffness change was simulated by changing elastic modulus of the materials and also changing spring constants of the link elements described in Fig. 4.

For each foundation condition, forced vibration analysis was performed by wave impact force. The caisson's stiffness change was simulated to comparatively estimate its effect on vibration responses. As shown in Fig. 17, maximum displacements of y and z directions were extracted at Extraction point 1 as stiffness changes were simulated on the caisson and the foundation (including armor stone, rubble mound, sand-fill, and natural ground). In all cases, the displacement was increased by the decrease of stiffness. The amount of displacement variation was larger in y-direction than in z-direction. The displacement variation was sensitively induced by the foundation change than the caisson change. Among all foundation components, the rubble mound was most sensitive to the displacement variation.

From the mode identification, two Modes Im 1 and Im 3 (which are identical to Modes Wp 1 and Wp 2) were extracted. Natural frequencies decreased gradually due to the stiffness decrease. Figure 18 shows the variation rate of natural frequency due to the change of the caisson and foundation. The foundation condition resulted in more sensitive changes in natural frequencies than the caisson condition. In Mode Im 1, stiffness changes in the sand fill and the rubble mound were more sensitive to the natural frequencies than the others. In Mode Im 3, stiffness changes in the sand fill and the natural ground were more sensitive than the others.

6.3.2 Relative impacts of foundations under uncertain waves and sea levels

As investigated previously, natural frequencies vary due to the variation of foundations, waves, and sea levels. However, their relative impacts were different as described in Figs. 15, 16, and 18, respectively. In this study, our interest is to distinguish the change of vibration characteristics of the caisson-foundation system induced by the change of foundation condition from that induced by the sea ambient conditions.

To account the wave-induced uncertainty on the foundation-induced change in vibration characteristics, the two modes Im 1 and Im 3 were comparatively analyzed from Fig. 15(b) and Fig. 18. Wave-induced variations of natural frequencies were 3.5% in Mode Im 1 and 5.5% in Mode Im 3. These can be equivalently accounted as the change in vibration responses induced by the change of foundation condition. The 3.5% in Mode Im 1 corresponds to the sand-fill's stiffness reduction of 7.7% or the rubble

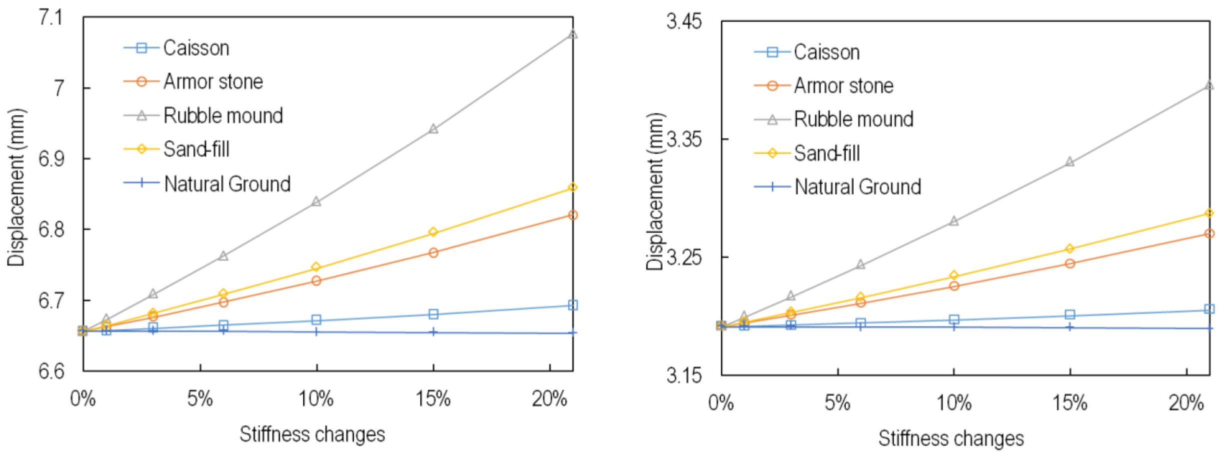

(a) Y-direction (b) Z-direction

Fig. 17 Variation rate of maximum displacement due to stiffness change of foundation

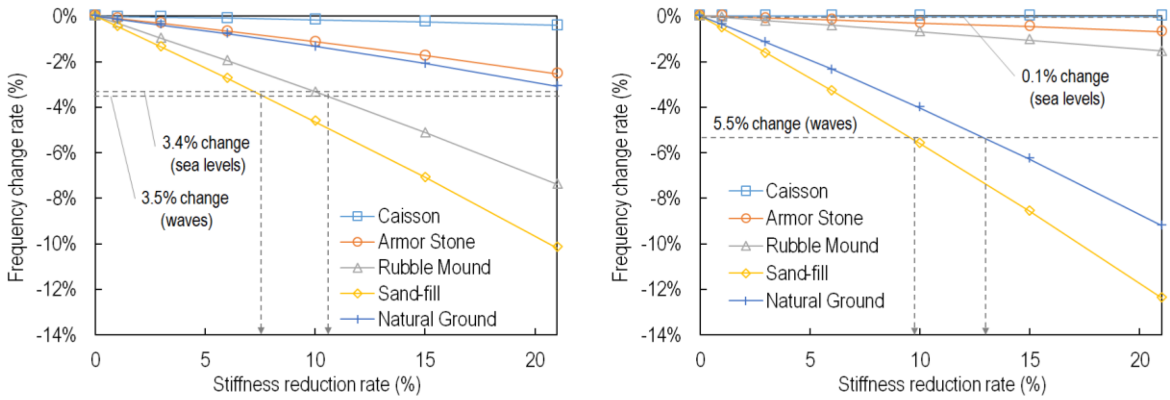

(a) Mode Im 1 (b) Mode Im 3

Fig. 18 Variation rate of natural frequencies due to stiffness change of foundation

Table 7 Scenarios of stiffness change in caisson and foundation components

Stiffness decrease	Elastic modulus (MPa)				Spring constant ($kg/m/m^2$)
	Caisson	Armor stone	Rubble mound	Sand fill	Natural ground
0%	2.80E+04	140	140	66.5	1.25E+07
1%	2.77E+04	138.6	138.6	65.835	1.24E+07
3%	2.72E+04	135.8	135.8	64.505	1.21E+07
6%	2.63E+04	131.6	131.6	62.51	1.18E+07
10%	2.52E+04	126	126	59.85	1.13E+07
15%	2.38E+04	119	119	56.525	1.06E+07
21%	2.21E+04	110.6	110.6	52.535	9.88E+06

mound's stiffness reduction of 10.8%. The 5.5% in Mode Im 3 corresponds to the sand-fill's stiffness reduction of 9.6% or the natural ground's stiffness reduction of 12.8%.

From Figs. 16 and 18, the sea level-induced uncertainty on the foundation-induced change in vibration characteristics was estimated by using the two modes Im 1 and Im 3. Sea level-induced variations of natural frequencies were 3.4% in Mode Im 1 and 0.1% in Mode Im 3. The 3.4% in Mode Im 1 corresponds to the sand-fill's stiffness reduction of 7.4% or the rubble mound's stiffness reduction of 10.2%. The 0.1% in Mode Im 3 corresponds to very small stiffness reduction of all foundation components. It is noted that the effect of the stiffness change in the sand-fill and the rubble mound of 7-8% can be overshadowed by variations of waves and sea levels when Mode Im 1 was utilized. It is also noted that the effect of the stiffness change in the sand-fill and the natural ground of 9-13% can be overshadowed by variations of waves and sea levels when

Mode Im 3 was utilized. Based on the numerical investigation, other components such as the armor stone and the caisson were relatively insensitive to vibration characteristics, so that the change in waves or sea levels would overshadow their effects.

7. Conclusions

In this study, vibration characteristics of a caisson-foundation breakwater system were investigated for ambient and geometric parameters such as various waves, sea levels and foundation conditions. Operational modal analysis methods which include time-domain and frequency-domain methods were selected to identify vibration modes from output-only dynamic responses. A finite element model of an existing caisson-foundation breakwater system was established by using a structural analysis program, ANSYS. Forced vibration analyses were performed on the caisson-foundation system for two types of external forces such as controlled impact and wave-induced dynamic pressure. For the ideal impact, the wave force was converted to a triangular impulse function. For the wave flow, the wave pressure acting on the system was obtained from wave field analysis. Vibration modes of the caisson-foundation system were identified from forced vibration responses by combined use of the operational modal analysis methods. Vibration characteristics of the caisson-foundation system were investigated under various waves, sea levels, and foundations. The relative effect of foundation condition on vibration characteristics was distinguished from that induced by waves and sea levels.

From the numerical examination on the caisson-foundation system, a few concluding remarks can be made as follows:

(1) The caisson-foundation system had complex vibrational behaviors consisting of caisson's rigid body motion and foundation's deformable motion. The foundation's behaviors could be investigated from vibration monitoring on the caisson.
(2) Vibration characteristics could be identified from wave-induced dynamic pressures, from which a few vibration modes represented caisson's rolling and foundation's flexural behaviors.
(3) Three components including sand-fill, rubble mound, and natural ground were sensitive to vibration characteristics in spite of their relatively contributions to vibration mode types. The ambient parameters such as waves and sea levels also contributed to the change of vibration characteristics.
(4) For vibration monitoring under ambient conditions, 7-13% of stiffness changes in the sensitive foundation components could be overshadowed due to the effects of waves and sea levels on vibration characteristics of the caisson-foundation system. The stiffness changes in the insensitive components might not be detectable when a few modes were utilized.
(5) Future works are remained to experimentally investigate the vibration characteristics of the caisson-foundation system under the real ambient conditions. In particular, the effect of complex wave conditions on the vibration characteristics should be investigated from laboratory and in-site tests.

Acknowledgments

This work was supported by the National Research Foundation of Korea (NRF) grant funded by the Korea government (MSIT) (NRF-2018R1A6A3A01013004).

References

Bowles, J.E. (1996), Foundation Analysis and Design, McGraw-Hill, 5th edition, Singapore.
Brincker, R., Zhang, L. and Andersen, P. (2001), "Modal identification of output-only systems using frequency domain decomposition", *Smart Mater. Struct.*, **10**(3), 441-445.
Brinker, R. and Andersen, P. (2006), "Understanding stochastic subspace identification", *Proceedings of the 24th International Modal Analysis Conference*, St. Louis, Missouri, January.
Catbas, F.N., Ciloglu, S.K., Hasancebi, O., Grimmelsman, K. and Aktan, A.E. (2007), "Limitations in structural identification of large constructed structures", *J. Struct. Eng.*, **133**(8), 1051-1066.
Cuomo, G., Lupoi, G., Shimosako, K., and Takahashi, S. (2011), "Dynamic response and sliding distance of composite breakwaters under breaking and non-breaking wave attack", *Coast. Eng.*, **58**(10), 953-969. doi: 10.1016/j.coastaleng.2011.03.008.
Ewins, D.J. (2000), "Modal Testing: theory, practice and application", 2nd edition, Research Studies Press Ltd., Hertfordshire, UK.
Galiatsatou, P., Makris, C. and Prinos, P. (2018), "Optimized reliability based upgrading of rubble mound breakwaters in a changing climate", *Marine Sci. Eng.*, **6**(92) doi:10.3390/jmse6030092.
Gao, M., Dai, G.Y. and Yang, J.H. (1988), "Dynamic studies on caisson-type breakwaters", *Proceedings of the 21st Conference on Coastal Engineering*, Torremolinos, Spain, June.
Gul, M. and Catbas, F.N. (2011), "Damage assessment with ambient vibration data using a novel time series analysis methodology", *J. Struct. Eng. - ASCE*, **137**(12), 1518-1526.
Ho, D.D., Stubbs, N., Park, W. and Kim, J.T. (2012), "Prestress-force estimation in PSC girder using modal parameters and system identification", *Adv. Struct. Eng.*, **15**(6), 997-1012. https://doi.org/10.1260/1369-4332.15.6.997.
Huynh, T.C., Lee, S.Y., Dang, N.L. and Kim, J.T. (2019), "Vibration-based structural identification of caisson-foundation system via in situ measurement and simplified model", *Struct. Control Health Monit.*, e2315. doi:10.1002/stc.2315.
KHOA (Korea Hydrographic and Oceanographic Agency) (2019), http://www.khoa.go.kr/koofs/eng/observation/obs_real_detail.do.
Kim, J.T. and Stubbs, N. (1995), "Model uncertainty impact and damage-detection accuracy in plate girder", *J. Struct. Eng. - ASCE*, **121**(10), 1409-1417. https://doi.org/10.1061/(ASCE)0733-9445(1995)121:10(1409).
Lamberti, A. and Martinelli, L. (1998), "Prototype measurements of the dynamic response of caisson breakwaters", *Proceedings of the 26th International Conference on Coastal Engineering, ASCE*, Copenhagen, Denmark, June.
Lee, S.Y., Huynh, T.C. and Kim, J.T. (2015), "Structural

identification of gravity-type caisson structure via vibration feature analysis", *Smart Struct. Syst.*, **15** (2), 259-281. http://dx.doi.org/10.12989/sss.2015.15.2.259.
Lee, S.Y., Huynh, T.C. and Kim, J.T. (2018), "A practical scheme of vibration monitoring and modal analysis for caisson breakwater", *Coast. Eng.*, **137**, 103-119. https://doi.org/10.1016/j.coastaleng.2018.03.008.
Lee, S.Y., Huynh, T.C., Kim, J.T., Yoon, H.S. and Han, S.H. (2013), "Vibration characteristics of gravity-type caisson breakwater structure with water-level variation", *Int. J. Distrib. Sens. N.*, **261396**. doi:10.1155/2013/261396.
Li, H.N., Yi, T.H., Ren, L., Li, D.S. and Huo, L.S. (2014), "Reviews on innovations and applications in structural health monitoring for infrastructures", *Struct. Monit. Maint.*, **1**(1), 1-45. http://dx.doi.org/10.12989/smm.2014.1.1.001
Overschee, V.P. and De Moor, B. (1996), "Subspace identification for linear system", *Kluwer Academic Publisher*, Dordrecht, Netherlands.
Schmidt, R., Oumeraci, H. and Partenscky, H.W. (1992), "Impact loads induced by plunging breakers on vertical structures", *Proceedings of the 23rd International Conference on Coastal Engineering*, Venice, Italy, October.
Shimoi, N., Saijo, M., Cuadra, C. and Madokoro, H. (2015), "Comparison of natural frequency vibration analysis for a bridge using accelerometers and a piezoelectric cable vibration sensor", *Int. J. Instrum. Sci.*, **4**(1). doi:10.5923/j. instrument.20150401.01.
Tagagi, H. (2015), "Method for quick assessment of caisson breakwater failure due to tsunamis: retrospective analysis of data from the 2011, Great East Japan Earthquake and Tsunami", *Coast. Eng.*, **57**(3). doi:10.1142/S057856341 5500126.
Vink, H.A.T. (1997), "Wave impacts on vertical breakwaters", Master's thesis, Faculty of Civil Engineering, Delft University of Technology, Netherlands.
Westergaard, H.M. (1933), "Water pressure on dams during earthquakes", *T. Am. Soc. Civil Engineers*, **98**(2), 418-433
Yi, J.H. and Yun, C.B. (2004), "Comparative study on modal identification methods using output-only information", *Struct. Eng. Mech.*, **17**(3-4), 445-446. https://doi.org/10.12989/sem.2004.17.3_4.445.
Yi, J.H., Park, W.S., Lee, S.Y., Huynh, T.C., Kim, J.T. and Seo, C.K. (2013), "Evaluation of vibration characteristics of an existing harbor caisson structure using tugboat impact tests and modal analysis", *Int. J. Distrib. Sens. N.*, **806482**. doi:10.1155/2013/806482.

HJ